Comparison between Wavenumber Truncation and Horizontal Diffusion Methods in Spectral Models

PETER C. CHU, XIONG-SHAN CHEN, AND CHENWU FAN

Department of Oceanography, Naval Postgraduate School, Monterey, California

ABSTRACT

Commonly used horizontal diffusion and wavenumber truncation dealiasing methods in spectral models are verified using the National Center for Atmospheric Research Community Climate Model version 3. For the same horizontal grid resolution, time step, physical processes, boundary conditions, and initial conditions, the simulated climate, using the horizontal diffusion alone model, is better than that using the wavenumber truncation method. In comparison with the observed climate data, the global root-mean-square of simulated January monthly mean 500-hPa geopotential using the horizontal diffusion alone model is 25% less than that using the wavenumber truncation model. However, for the same spectral resolution, the wavenumber truncation model (high horizontal grid resolution) leads to more accurate solutions than the horizontal diffusion model (low horizontal grid resolution).

1. Introduction

Silberman (1954) introduced the spectral method in meteorological modeling, solving the nondivergent barotropic vorticity equation using an interaction coefficient method to calculate the nonlinear terms. Platzman (1960), Bear and Platzman (1961), Kubota et al. (1961), and Ellsaesser (1966) also discussed the integration of the vorticity equation using the same method. This method, however, was not practical for operational use due to the considerable computational power needed to calculate the nonlocal sums of the nonlinear terms. This problem was solved by Eliasen et al. (1970), Orszag (1970, 1971), and Machenhauer and Rasmussen (1972) by using the transform method. The method involves the inverse transform of model variables from spectral space to physical space, the computation of nonlinear advection terms at grid points, and the transform of the nonlinear terms to spectral space.

The nonlinear instability was first studied by Phillips (1959), who found that the cause of this instability is aliasing. The short wavelength of the waves to be represented on the grid is 2Δ (where 2Δ is the grid size), but the waves generated by the nonlinear terms (from the advection term) may have wavelengths of less than 2Δ. Thus, the generated waves with wavelengths of less than 2Δ must be falsely represented (or aliased) by the

waves with longer wavelength (of which most are 2Δ or 4Δ). This computational phenomenon is referred to as aliasing. Repeated aliasing over many times may give rise to rapid growth of wave energy in wavelengths 2Δ and 4Δ and causes the nonlinear instability.

The nonlinear instability occurs not only in spectral models but also in finite-difference models and was originally found in a finite-difference model by Phillips (1959). Phillips suggested that the nonlinear instability could be controlled by periodically removing wavelengths 4Δ and smaller by using a Fourier analysis, or by application of a space filter, or by inclusion of an artificial horizontal diffusion term. Several methods were proposed to avoid the nonlinear instability: 1) the horizontal diffusion method (Phillips 1959), 2) the wavenumber truncation method (Orszag 1970, 1971; Machenhauer and Rasmussen 1972), and 3) the enstrophy conserved difference scheme (Arakawa 1966). The first two methods are commonly used in spectral models. The horizontal diffusion method uses a sufficiently larger value to suppress the nonlinear instability. The wavenumber truncation method uses the $3M + 1$ point discrete Fourier transform in the transform method to obtain the nonlinear term in the $2M + 1$ point discrete Fourier transform, where M is the maximum truncated wavenumber of the solution. In fact, this method is to remove or to truncate the high wavenumbers from the solution to prevent the nonlinear instability. In current spectral and finite-difference models, several of the above methods are used at the same time, or at least one of the above methods is used to suppress the nonlinear instability.

Corresponding author address: Dr. Peter C. Chu, Department of Oceanography, Naval Postgraduate School, Monterey, CA 93943. E-mail: chu@nps.navy.mil

Report Documentation Page

Public reporting burden for the collection of information is estimated to average 1 hour per response, including the time for reviewing instructions, searching existing data sources, gathering and maintaining the data needed, and completing and reviewing the collection of information. Send comments regarding this burden estimate or any other aspect of this collection of information, including suggestions for reducing this burden, to Washington Headquarters Services, Directorate for Information Operations and Reports, 1215 Jefferson Davis Highway, Suite 1204, Arlington VA 22202-4302. Respondents should be aware that notwithstanding any other provision of law, no person shall be subject to a penalty for failing to comply with a collection of information if it does not display a currently valid OMB control number.

1. REPORT DATE **MAY 2000**	2. REPORT TYPE	3. DATES COVERED **00-00-2000 to 00-00-2000**

4. TITLE AND SUBTITLE **Comparison Between Wavenumber Truncation and Horizontal Diffusion Methods in Spectral Models**	5a. CONTRACT NUMBER
	5b. GRANT NUMBER
	5c. PROGRAM ELEMENT NUMBER
6. AUTHOR(S)	5d. PROJECT NUMBER
	5e. TASK NUMBER
	5f. WORK UNIT NUMBER
7. PERFORMING ORGANIZATION NAME(S) AND ADDRESS(ES) **Naval Postgraduate School ,Department of Oceanography,Monterey,CA,93943**	8. PERFORMING ORGANIZATION REPORT NUMBER
9. SPONSORING/MONITORING AGENCY NAME(S) AND ADDRESS(ES)	10. SPONSOR/MONITOR'S ACRONYM(S)
	11. SPONSOR/MONITOR'S REPORT NUMBER(S)

12. DISTRIBUTION/AVAILABILITY STATEMENT
Approved for public release; distribution unlimited

13. SUPPLEMENTARY NOTES

14. ABSTRACT

15. SUBJECT TERMS

16. SECURITY CLASSIFICATION OF:			17. LIMITATION OF ABSTRACT	18. NUMBER OF PAGES	19a. NAME OF RESPONSIBLE PERSON
a. REPORT **unclassified**	b. ABSTRACT **unclassified**	c. THIS PAGE **unclassified**	**Same as Report (SAR)**	**7**	

In current spectral models such as the National Center for Atmospheric Research (NCAR) Community Climate Model version 3 (CCM3) and the European Centre for Medium-Range Weather Forecasts (ECMWF) model, both the horizontal diffusion method and the wavenumber truncation method are used to prevent the aliasing and nonlinear instability. In general, if the wavenumber truncation method is deleted in the current CCM3, the larger coefficients of the horizontal diffusion need to be used to prevent the aliasing, and, on the contrary, if the horizontal diffusion method is deleted, a stronger wavenumber truncation method needs to be used in the model. One problem emerges: What happens if only one method (horizontal diffusion or wavenumber truncation) is used in the spectral model? We will study this problem here using the CCM3. The outline of the paper is as follows. In section 2, we describe the climate spectral model using CCM3. In sections 3 and 4, we discuss the performance of the wavenumber truncation method only and the horizontal diffusion method only, respectively. In section 5, we compare between the two dealiased methods in climate simulation. In section 6, we present the conclusions.

2. Climate spectral models

a. Model description

The CCM3 evolved from the Australian spectral model described by Bourke et al. (1977) and McAvaney et al. (1978). The CCM3 uses both wavenumber truncation and horizontal diffusion methods to suppress the nonlinear instability. The wavenumber truncation method is used to remove the highest one-third wave components. The horizontal diffusion method is used for temperature, vorticity, and divergence with the default values: $\varepsilon_0 = 0.06$ for the time filter, $K_0^{(2)} = 0.25 \times 10^6$ m^2 s^{-1} for the horizontal diffusion in a linear ∇^2 form in the top three levels of the model, and $K_0^{(4)} = 1.0 \times 10^{16}$ m^4 s^{-1} for a linear biharmonic ∇^4 form at all other levels. The time step in this study is taken as $\Delta t = 20$ min.

b. Initial and boundary conditions

The initial data used in this study are for the 1 September climatology of the atmospheric and surface fields, provided by the NCAR Climate and Global Dynamics (CGD) Division. The initial data include temperature T, zonal wind component u, meridional wind component v, water vapor specific humidity q, surface geopotential ϕ_s, surface pressure p_s, and four subsurface temperatures T_s.

The time-invariant boundary data are surface albedo, orography, surface aerodynamic roughness over land, surface evaporation factor, vegetation type, January snow cover, and July snow cover. The time-varying boundary data include the sea surface temperature, which contains 12 months of data as 12 time samples, and the ozone volume mixing ratios.

c. Nomenclature

We use TXXGYY(ε, $K^{(2)}$, $K^{(4)}$) to identify each model run with the maximum wavenumber (XX), the grid points around a latitude cycle (YY), the time filter (ε), and horizontal diffusion coefficients ($K^{(2)}$, $K^{(4)}$). For example, the CCM3 spectral model T21G64 with default values of the time filter (ε) and horizontal diffusion coefficients ($K^{(2)}$, $K^{(4)}$) can be represented by T21G64(ε_0, $K_0^{(2)}$, $K_0^{(4)}$). It has 32 Gaussian latitudes from the South Pole to the North Pole and 18 vertical levels with a top at 2.917 hPa, triangular truncation with the maximum wavenumber 21, and 64 grid points around a latitude circle (approximately a 5.6° × 5.6° transform grid and 64 × 32 × 18 grid points).

d. Experiment design

We design the following experiments to verify the wavenumber truncation method and the horizontal diffusion method in spectral modeling: 1) the wavenumber truncation method only (i.e., $K^{(2)} = K^{(4)} = \varepsilon = 0$), 2) the horizontal diffusion method only (keeping all the wave components), and 3) both the wavenumber truncation and horizontal diffusion methods present but with different spectral resolutions.

For the type-1 experiments, we integrate the two spectral models:

$$W1 = T21G64(0, 0, 0) \quad \text{and} \quad W2 = T16G64(0, 0, 0).$$

For the type-2 experiments, we integrate the three spectral models:

$$H1 = T31G64(\varepsilon_0, K_0^{(2)}, K_0^{(4)}),$$

$$H2 = T31G64(\varepsilon_0, 2K_0^{(2)}, 2K_0^{(4)}), \quad \text{and}$$

$$H3 = T31G64(\varepsilon_0, 7K_0^{(2)}, 7K_0^{(4)}).$$

For the type-3 experiments, we integrate the three spectral models:

$$R1 = T21G64(\varepsilon_0, K_0^{(2)}, K_0^{(4)}),$$

$$R2 = T21G64(\varepsilon_0, 7K_0^{(2)}, 7K_0^{(4)}), \quad \text{and}$$

$$R3 = T31G96(\varepsilon_0, K_0^{(2)}, K_0^{(4)}).$$

e. Model output

1) GLOBAL STATISTICS

The CCM3 model computes the global statistics at each time step for diagnostic purposes: root-mean-square (rms) divergence, RMSD (s^{-1}); rms absolute vorticity, RMSZ (s^{-1}); rms temperature, RMST (K); mass integral, STPS (Pa); moisture integral, STQ (kg m^{-2}); the maximum Courant number for the horizontal velocity field, HOR (dimensionless); the maximum Courant number for the vertical velocity field, VERT (dimensionless).
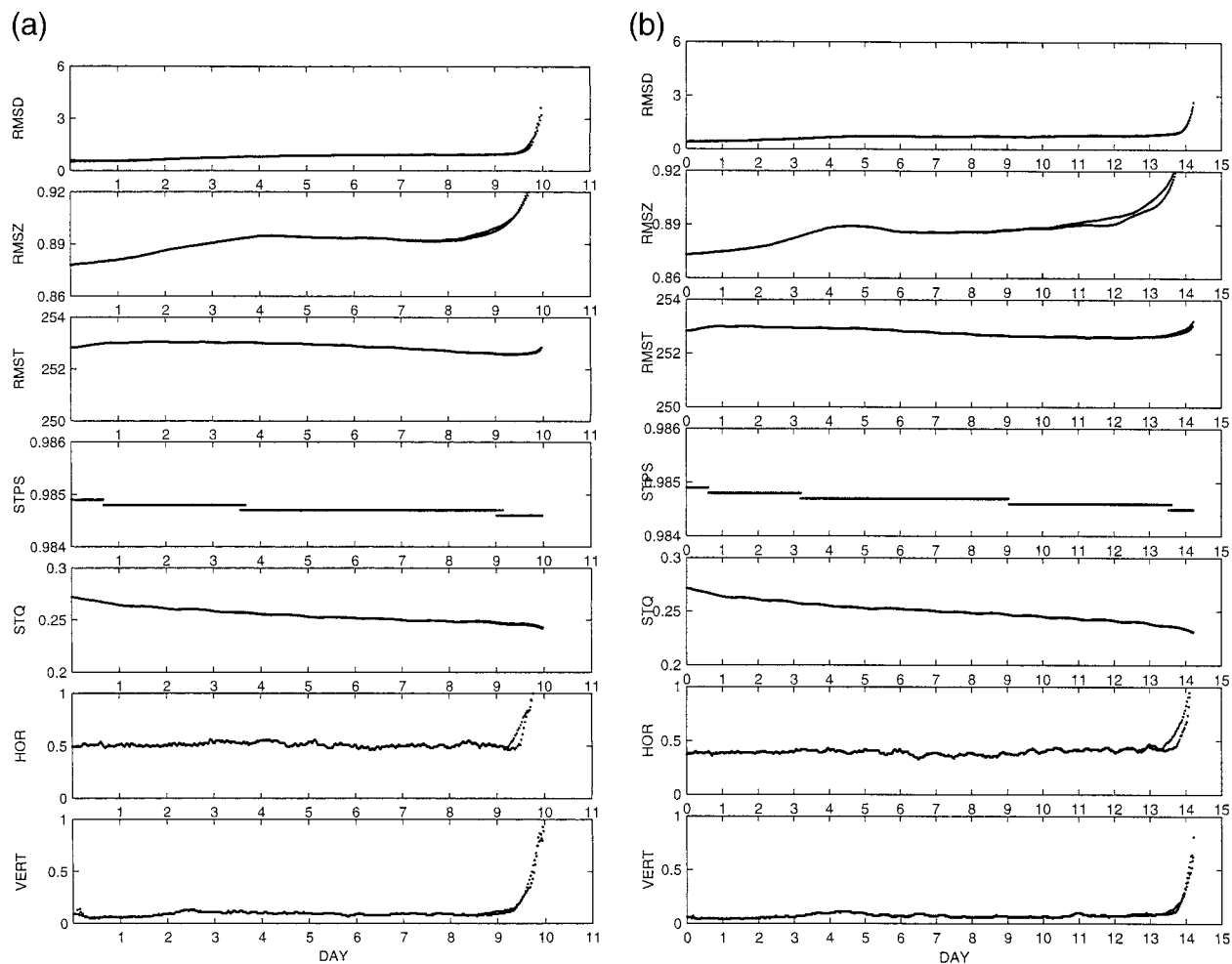
(a)

(b)

FIG. 1. Temporally varying global statistics for type-1 (wavenumber truncation) experiments (a) W1 and (b) W2: RMSD (in 10^{-5} s^{-1}), RMSZ (in 10^{-4} s^{-1}), RMST (in K), STPS (in 10^5 Pa), STQ (in 10^2 kg m^{-2}), HOR (dimensionless), and VERT (dimensionless).

2) MONTHLY MEAN 500-HPA GEOPOTENTIAL FIELDS

Four of the above seven spectral models—H3, R1, R2, R3—are selected for the comparison of the monthly mean 500-hPa geopotential fields. We integrate the four models (H2, R1, R2, R3) from the initial climatological data (1 Sep) for 2 yr and compute the monthly mean 500-hPa geopotential fields from the model output.

We use the ECMWF Reanalysis sample data for 1979–93 for model verification. Since the four models (H3, R1, R2, R3) in this study simulate the annual variation of the atmospheric fields, we average the ECMWF Reanalysis synoptic sample data over 1979–93 to obtain the climatological monthly mean data for verifying the model results.

3. Wavenumber truncation method

To verify the importance of the wavenumber truncation method, we integrate the W1 and W2 models and

show the results in Fig. 1a for W1 and Fig. 1b for W2. The parameters HOR and VERT exceed 1.0 at the 732d time step (equivalent to 10 days) in the W1 and at 1023d time step (equivalent to 14 days) in the W2, and both models blow up. This indicates that use of the wavenumber truncation method alone cannot suppress all the nonlinear instability.

4. Horizontal diffusion method

To verify the importance of the horizontal diffusion method, we integrate the H1 and H2 models and show the results in Fig. 2a for H1 and Fig. 2b for H2. The parameters HOR and VERT in the H1 exceed 1.0 at the 144th time step (equivalent to 2 days), and the model blows up. As we double the horizontal diffusion coefficients (H2 model), the parameters HOR and VERT are always less than 1.0 (computationally stable); however, the model output contains high-frequency noises.
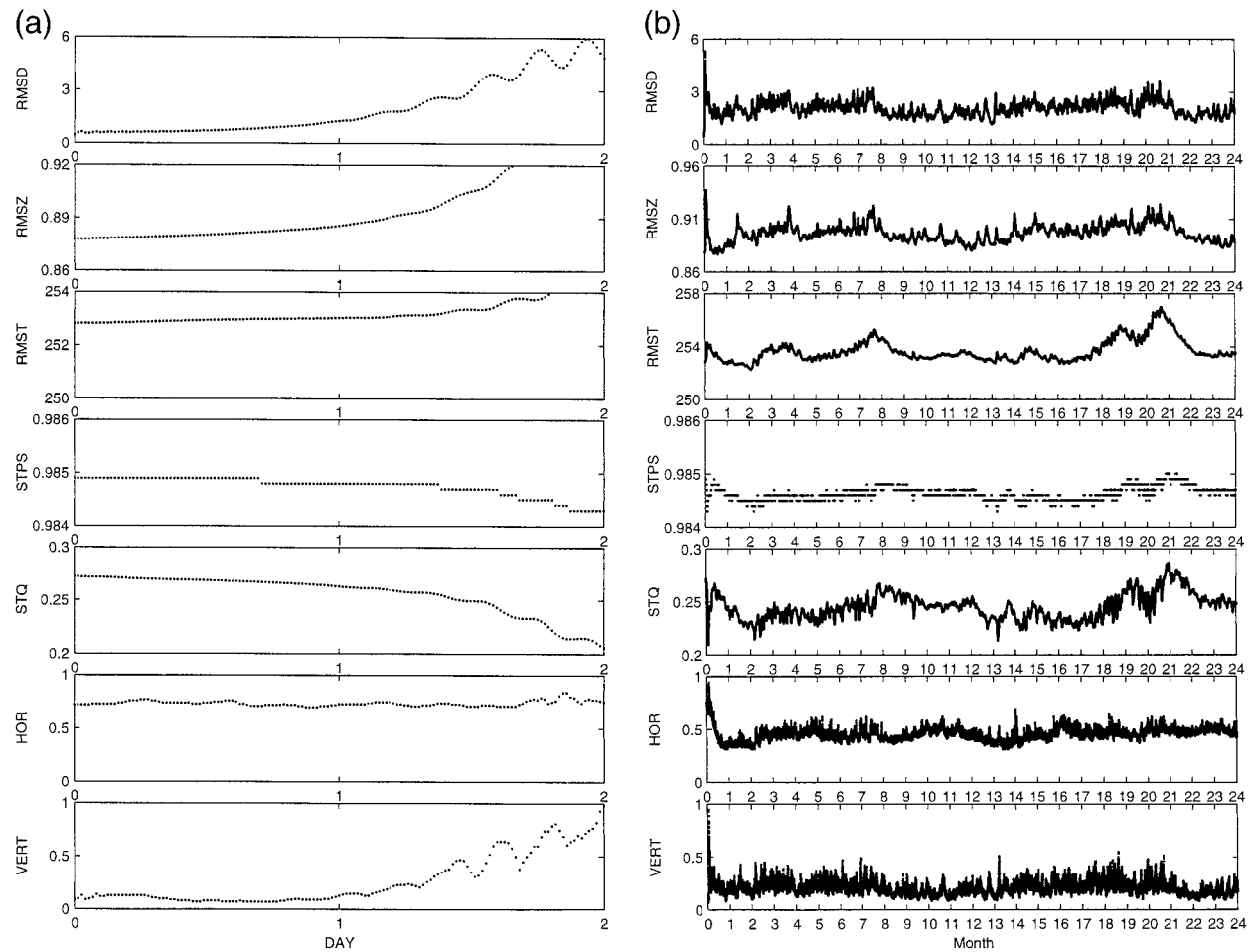
FIG. 2. Temporally varying global statistics for type-2 (horizontal diffusion) experiments (a) H1 and (b) H2: RMSD (in 10^{-5} s^{-1}), RMSZ (in 10^{-4} s^{-1}), RMST (in K), STPS (in 10^5 Pa), STQ (in 10^2 kg m^{-2}), HOR (dimensionless), and VERT (dimensionless).

5. Comparison among four stable models

Following is the comparison among the four stable model runs: H2, R1, R2, and R3.

a. Monthly mean 500-hPa geopotential fields

Each model has two simulated January and two simulated July fields. We compare the second simulated January and July with the monthly mean ECMWF data (taken as the "observed" data). The comparison is conducted in two subgroups: (a) same grid resolution (H3, R1, R2), and (b) same spectral resolution (H3, R3).

1) Models with the same grid resolution (H3, R1, R2)

Figure 3 shows the observed and the model-simulated monthly mean January 500-hPa geopotentials. The troughs of east Asia and the east coast of North America are well simulated in strength and in location in the H3

model. The simulated troughs in the R1 and R2 models are weaker in strength. The trough of the Middle East is well simulated in all the climate models in comparison with the observed data. In the Southern Hemisphere, the straight jet stream is well simulated in the H3 model, but the jet streams in the R1 and R2 models are too weak and meandering.

Figure 4 shows the observed and the model-simulated monthly mean July 500-hPa geopotentials. In the Northern Hemisphere, the ridge of North America is well simulated in the three models. In the Southern Hemisphere the jet stream is too strong in the H3 model and is too weak in the R1 and R2 models. The observed geopotential field shows a deep low with a geopotential contour of 47 600 m^2 s^{-2} near the South Pole. The H3 model (horizontal diffusion alone) simulates this deep low very well with the same contour (47 600 m^2 s^{-2}) at the same location (near the South Pole). However, the R1 and R2 models fail to simulate this system.
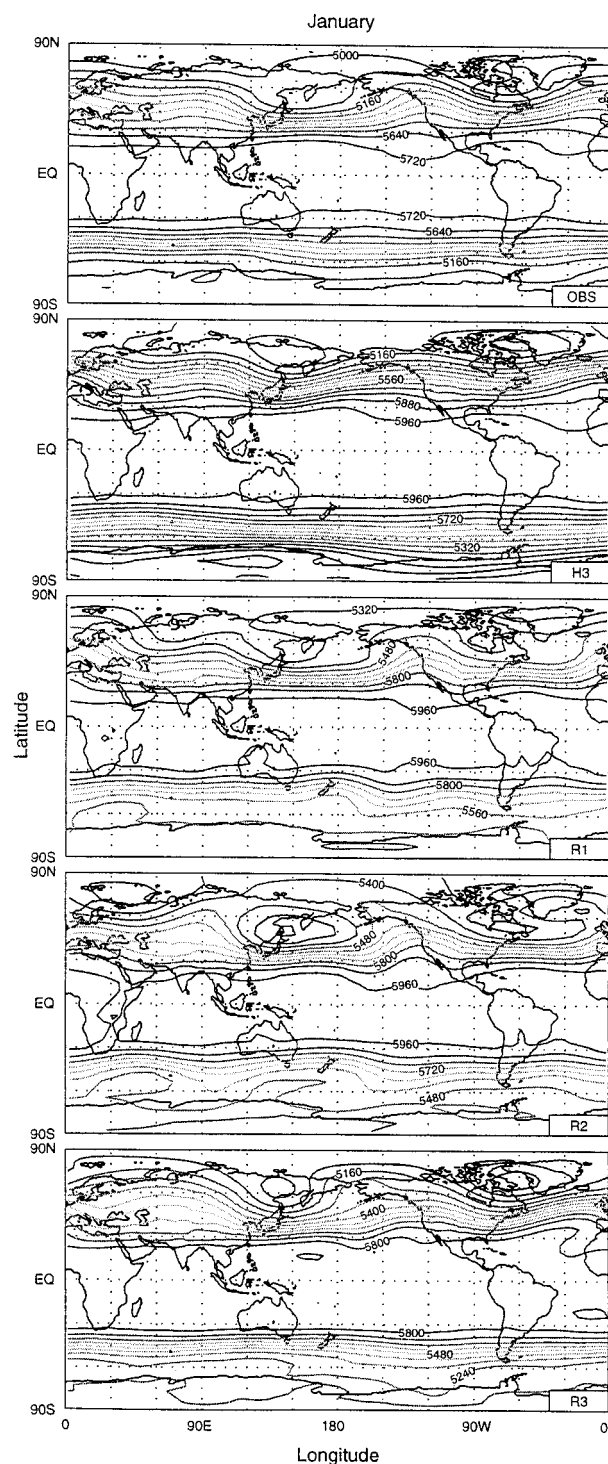
January

July

FIG. 3. The observed and simulated by stable models (H3, R1, R2, R3) Jan monthly mean 500-hPa geopotentials (in 10 m² s⁻²).

FIG. 4. The observed and simulated by stable models (H3, R1, R2, R3) Jul monthly mean 500-hPa geopotentials (in 10 m² s⁻²).

2) MODELS WITH THE SAME SPECTRAL RESOLUTION (H3, R3)

Both H3 and R3 in January have the same spectral resolution with the maximum wavenumber 31. The sim-
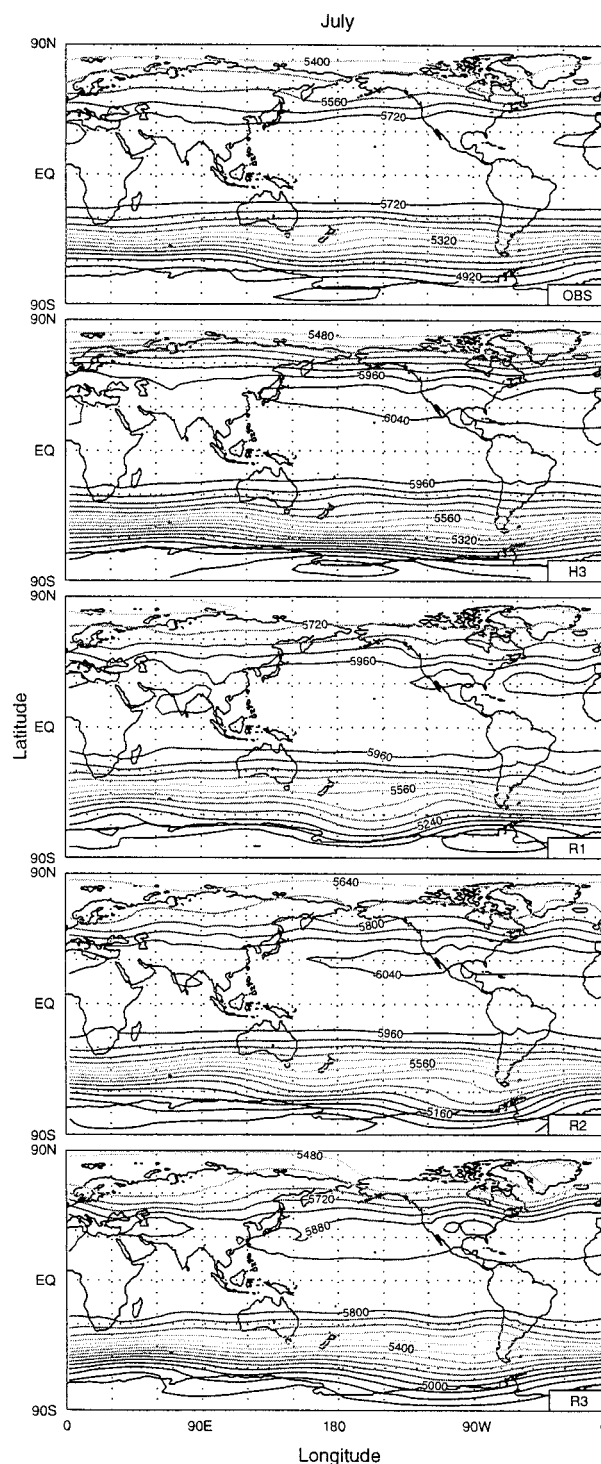
ulated troughs of east Asia and the east coast of North America in the R3 model are weaker in strength than in the H3 model. The trough of the Middle East is well simulated in the H3 model but not in the R3 model. In
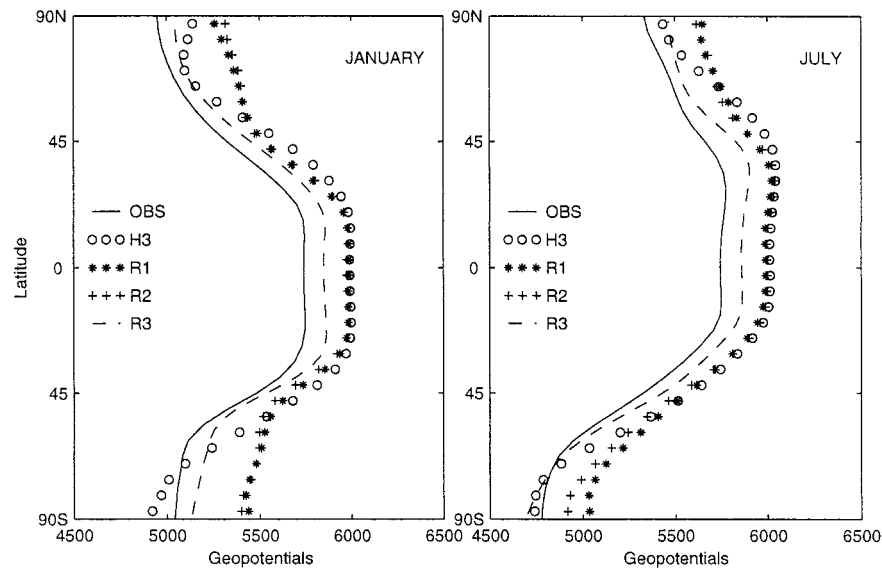
FIG. 5. The Jan and Jul meridional cross sections of the observed and the simulated zonal-averaged monthly mean 500-hPa geopotentials (in 10 m^2 s^{-2}).

the Southern Hemisphere, the straight jet stream is well simulated in both the H3 and R3 models with comparable strength to the observed field (Fig. 3).

In the Northern Hemisphere, the ridge of North America in July (Fig. 4) is well simulated in both models. In the Southern Hemisphere, the jet stream is too strong in the H3 model and is quite reasonable in the R3 model. The observed geopotential field shows a deep low with a geopotential contour of 47 600 m^2 s^{-2} near the South Pole. The H3 model simulates this deep low very well with the same contour (47 600 m^2 s^{-2}) at the same location (near the South Pole). However, the R3 model fails to simulate this system.

b. Zonally averaged monthly mean 500-hPa geopotentials

We compute the zonally averaged monthly mean 500-hPa geopotentials. From the meridional cross sections of the zonal-averaged monthly mean 500-hPa geopotentials (Fig. 5), we find that among the same grid resolution models (H3, R1, R2) the H3 model-simulated values are much closer to the observed data than the other two (R1, R2) model-simulated values, especially in the middle and high latitudes.

For the same grid resolution, comparable values simulated using R1 to using R2 (same wavenumber truncation but different horizontal diffusion coefficients) implies the insensitivity of model results to horizontal diffusion coefficients. Improvement of the simulation (especially in high latitudes) using H3 compared to using R2 (same large horizontal diffusion coefficients but different spectral resolution) indicates that a high spectral resolution (untruncated model) leads to a high model accuracy. For the same spectral resolution, the high grid-resolution model (R3) simulates values closer to the observed values than the H3 model although it consumes much more computer time. Thus, both the grid resolution and the spectral resolution are key issues in determining the spectral model accuracy.

Tables 1 and 2 indicate the rms errors of the monthly mean 500-hPa geopotentials between observed and simulated values for the globe, the Northern Hemisphere, and the Southern Hemisphere, respectively. Among the same grid resolution models (H3, R1, R2), the horizontal diffusion alone model (H3) has the least errors in simulating climatological 500-hPa fields. Such an improvement is more evident in January than in July. In January, the rms errors of the H3 model for the globe, the Northern Hemisphere, and the Southern Hemisphere are 2160,

TABLE 1. Root-mean-square error of Jan mean 500-hPa geopotentials (in 10 m^2 s^{-2}).

Model	Global	Northern Hemisphere	Southern Hemisphere
H3	216	234	199
R1	289	276	300
R2	281	275	286
R3	106	109	104

TABLE 2. Root-mean-square error of Jul mean 500-hPa geopotentials (in 10 m^2 s^{-2}).

Model	Global	Northern Hemisphere	Southern Hemisphere
H3	228	253	203
R1	260	255	265
R2	238	258	216
R3	103	118	87

2340, and 1990 m^2 s^{-2}, respectively. These values are a 25%, 15%, and 34% error reduction compared to that of the R1 model and are a 23%, 15%, and 30% error reduction compared to that of the R2 model. In July, the rms errors of the H3 model for the globe, the Northern Hemisphere, and the Southern Hemisphere are 2280, 2530, and 2030 m^2 s^{-2}. These values are a 12%, 1%, and 23% error reduction compared to that of the R1 model, and are a 4%, 2%, and 6% error reduction compared to that of the R2 model, respectively. This indicates an encouraging improvement in the climate simulation using the horizontal diffusion alone method among the same grid resolution model. For the same spectral resolution models (H3 and R3), the high grid resolution model (R3) leads to a more accurate solution.

6. Conclusions

Our conclusions are as follows.

1) The capability of horizontal diffusion and wavenumber truncation dealiasing methods to suppress nonlinear instability in spectral models is investigated using the NCAR CCM3 model. The wavenumber truncation method alone cannot suppress the nonlinear instability even half of the wavenumbers are truncated. The horizontal diffusion method alone can suppress the nonlinear instability when the horizontal diffusion coefficients exceed some critical values.

2) When the horizontal diffusion coefficients ($K^{(2)}$, $K^{(4)}$) are taken at twice the CCM3's default values (0.25 $\times$ 10^6 m^2 s^{-1}, 1.0 $\times$ 10^{16} m^4 s^{-1}), the horizontal diffusion alone model is computationally stable, but the solution contains high-frequency noises. Increase of the horizontal diffusion coefficients leads to filtration of high-frequency noises.

3) Both the grid resolution and the spectral resolution are key issues in determining the spectral model accuracy. For the same grid resolution, the simulated climatological monthly mean fields are relatively insensitive to horizontal diffusion coefficients and are improved using an untruncated model (i.e., highest spectral resolution), when the diffusion coefficients are sufficiently large. For the same spectral resolution, the high grid resolution model leads to a more accurate simulation. This implies the importance of the wavenumber truncation method.

REFERENCES

Arakawa, A., 1966: Computational design for long-term numerical integrations of the equations of atmospheric motion. *J. Comput. Phys.,* **1,** 119–143.

Bear, F., and G. W. Platzman, 1961: A procedure for numerical integration of the spectral vorticity equation. *J. Meteor.,* **18,** 393–401.

Bourke, W., B. McAvaney, K. Puri, and R. Thurling, 1977: Global modeling of atmospheric flow by spectral methods. *Methods Comput. Phys.,* **17,** 267–324.

Eliasen, E., B. Machenhauer, and E. Rasmussen, 1970: On the numerical method for integration of hydrodynamical equation with a spectral representation of the horizontal fields. Institute of Theoretical Meteorology Rep. 2, University of Copenhagen, 37 pp.

Ellsaesser, H. W., 1966: Evaluation of spectral versus grid methods of hemispheric numerical weather prediction. *J. Meteor.,* **5,** 246–262.

Kubota, S., M. Hirose, Y. Kikuchi, and Y. Kurihara, 1961: Barotropic forecasting with the use of surface spherical harmonic representations. *Pap. Meteor. Geophys.,* **12,** 199–215.

Machenhauer, B., and E. Rasmussen, 1972: On the integration of the spectral hydrodynamical equation by a transform method. Institute of Theoretical Meteorology Rep. 3, University of Copenhagen, 44 pp.

McAvaney, B. J., W. Bourke, and K. Puri, 1978: A global spectral model for simulation of the general circulation. *J. Atmos. Sci.,* **35,** 1557–1583.

Orszag, S. A., 1970: Transform method for the calculation of vector-coupled sums: Application to the spectral form of the vorticity equation. *J. Atmos. Sci.,* **27,** 890–895.

——, 1971: Numerical simulation of incompressible flows within simple boundaries. I. Galerkin (spectral) representations. *Stud. Appl. Math.,* **50,** 293–327.

Phillips, N. A., 1959: An example of non-linear computational instability. *The Atmosphere and the Sea in Motion, Rossby Memorial Volume,* E. Bolin, Ed., Rockefeller Institute Press, 501–504.

Platzman, G. W., 1960: The spectral form of the vorticity equation. *J. Meteor.,* **17,** 635–644.

Silberman, I., 1954: Planetary waves in the atmosphere. *J. Meteor.,* **11,** 27–34.